J. Chem. Sci. Vol. 125, No. 6, November 2013, pp. 1607–1618.

Adsorption of parent nitrosamine on the nanocrystaline M-ZSM-5 zeolite: A density functional study

HOSSEIN ROOHI* and MAHJOUBEH JAHANTAB

Department of Chemistry, Faculty of Science, University of Guilan, Rasht, Iran
e-mail: hroohi@guilan.ac.ir

MS received 5 December 2012; revised 16 March 2013; accepted 5 April 2013

Abstract. The adsorption of parent nitrosamine (**NA**) on the Brønsted acid sites of M-ZSM-5 (M = H, Li and Na) zeolites have been investigated via the utilization of 10T cluster model by density functional calculations, at the B3LYP/6–311++G(d,p) level. Two **A** and **B** complexes with two types O(N)$\cdots$M and NH$\cdots$O$_Z$ interactions were predicted from adsorption of nitrosamine on the M-zeolite clusters. The comparison of interaction energies shows that the order of energies for adsorption of **NA** on the Brønsted acid site of M-ZSM-5 is Na < Li < H for the **A** complexes and Li < H for the **B** complexes. The calculated adsorption enthalpy of **NA** on the Brønsted acid site of 10T cluster of M-ZSM-5 catalyst ranges from −14.41 to −52.95 kJ/mol. The acid strength of H-ZSM-5 was found to exceed those of the corresponding to the alkali metal ion-exchanged zeolites. The results reveal that the interaction between hydrogen of **NA** and O$_Z$ of framework is weaker than O(N)$\cdots$M one. The NH$\cdots$O$_Z$ and O(N)$\cdots$H$_Z$ hydrogen bonds in these complexes are electrostatic and partially covalent in nature, respectively. The results of natural bond orbital (NBO) analysis showed that charge transfer occurs from **NA** to M-zeolite cluster.

Keywords. Adsorption; 10T cluster model; nitrosamine-M-zeolite complexes; NBO; AIM.

1. Introduction

Approximately 60–90% of human cancers are attributed to environmental factors, particularly chemical carcinogens. Nitrosamines along with mycotoxins are two important groups of carcinogens that have been emerged.[1,2] Nitrosamines are also well-recognized teratogens and carcinogens in animals and are considered potentially carcinogenic in humans. With a characteristic functional group of –N–N=O in their structure, nitrosamines can cause serious health risk and they can induce cancer or tumours even in trace amounts.[3–6] Nitrosamines are probably the most widespread carcinogens in the workplace, processed meats, cigarette smoke, bacon and beer.[6,7] In addition, volatile nitrosamines are also found in the vapour or semivolatile phase of mainstream smoke inhaled by smokers.[8]

Zeolites are microporous crystalline materials with high surface areas composed of TO_4 (T = Si, Al) tetrahedral as primary units joined via oxygen to give cage like structures.[9] Because of their shape–selectivity and Brønsted acidity, zeolites have found important applications in chemical separations, catalysis and adsorption. Various molecules such as alkenes,[10] NH_3,[11,12] methanol,[13] 4,4′-Bipyridine,[14] CO, NO and N_2O[15–19] and chlorofluorocarbons (CFC)[20] have been reported to be absorbed by zeolites. To balance the excess of charges when substitutions of silicon with aluminum occur, cations are present.[21–25] Cation zeolites can be converted to protonic zeolites; then, one obtains solid acid catalyst.[26]

The ZSM-5 zeolite, characterized by a three-dimensional pore system with straight and sinusoidal channels, possesses unique channel structure, thermal and hydrothermal stability and acidity.[27] As is known, there are 12 crystallographically distinct tetrahedral states (T-sites) occupied by Si or Al atoms in the orthorhombic form of ZSM-5 zeolites.[28] These T-sites are numbered as T1–T12. The T12 site should be located preferentially at the intersections of straight and zigzag channels in zeolites; hence, it is believed to be one of the more active sites in ZSM-5.[27] There have been several previous theoretical studies on the adsorption of various molecules on different sites in ZSM-5 zeolite.[27,29–32]

To selectively remove the nitrosamines, zeolites are considered as the candidates because of their ability

*For correspondence

of selective adsorption and catalysis functions. Nitrosamines are assumed to adsorb by inserting the –N–N=O group into the channel of the zeolites.[33,34] Zeolites are able to adsorb the nitrosamines in solution, and the equilibrium adsorption isotherms correlate with the Freundlich equation. The adsorption capacity of zeolites mainly depended on their pore size, surface area and acid–base properties.[34–36] Adsorption of various nitrosamines on the zeolites has been investigated experimentally.[1,4,37–39] Also, zeolites can efficiently trap the volatile nitrosamines in gas stream at ambient temperature even though the contact time was shorter than 0.1 s.[7,40] Zeolite ZSM-5 is one of the most useful catalysts that have been widely used in the adsorption of serious pollutants.[1,7,15,18,34,35,38]

In our recent paper,[41] the ONIOM method was employed for investigating the adsorption of parent nitrosamine over H-ZSM-5 zeolite. In this present paper, we investigate the effect of cation exchange on the acid strength of M-ZSM-5 zeolite (M = Li and Na) on the adsorption of the NA, using the density functional calculations (DFT). In the alkali metal exchanged zeolites there are two types of active sites: (i) the alkali metal cations can act as Lewis acid sites and (ii) the zeolite framework oxygen atoms can act as basic sites.[29] **NA** can interact with both types of active sites: **NA** interacts with an alkali metal cation and hydrogen of N–H group of **NA** can form a hydrogen bond (H-bond) with framework oxygen atoms. Both of these effects influence the N=O and N–H bond; therefore, their stretching frequency is changed. Interaction between 10T cluster models of M-ZSM-5 with **NA** is studied structurally, energetically, and topologically. We also compare our results obtained in the alkali metal cation exchanged zeolites and H-ZSM-5 to determine the effect of ion exchange on the acid strength of them.

2. Method and model

The cluster models 10T, which are a part of the framework at the main channel of the zeolite have molecular structure of $[AlSi_9O_{12}H_{20}]^-M^+$.[42–44] The label on the model refers to the number of tetrahedrally coordinated atoms, T atoms, that is Si and Al atoms in model. Also, in model cluster, an aluminum atom replaces a silicon atom (9 tetrahedral atoms of Si and 1 tetrahedral atom of Al) and the resulting negative charge is compensated by H^+, Li^+ and Na^+ to produce M-zeolite (M = H, Li and Na) cluster (see figure 1). The peripheral bonds of the Si atoms were saturated with hydrogen atoms. The active site O–Al–O has been used in many theoretical studies.[45] To mimic the geometry constrains of the real zeolite structure, the Cartesian coordinates of boundary H atoms in clusters were held froze in all geometry optimization. The rest of the clusters have been fully optimized. The equilibrium distances were obtained by free cluster optimizations of similar cluster models.

The geometry optimizations of the NA–10T complexes were performed by Gaussian 03 program package.[46] All calculations were carried out at the B3LYP/6–311++G(d,p) level of theory, which is well-known for its consistency and reliability for zeolite systems.[15] Vibrational frequency calculations have been performed at the B3LYP/6–311++G(d,p) level of theory on the structures optimized at the same level to characterize stationary points and calculation of the zero-point and thermal energies.

It is well-known that the B3LYP have limitations for taking the dispersive energy into account.[47,48] However, computational capabilities of DFT, particularly B3LYP functional, in the study of zeolite systems have been reported in the literature.[10,14,27,29,30,45] In medium-strength HB interactions (such as systems studied here), the dispersion forces are a minor component of the adsorption energy. Therefore, B3LYP hybrid functional with a suitable basis set (6–311++G(d,p)) is expected to predict reasonably accurate interaction energies. But, calculated value of interaction energy by DFT methods in systems including weak interactions is smaller than experimental value and values obtained by high levels of theory. The failure to achieve agreement is not surprising because the accuracy of DFT methods is particularly poor for weakly adsorbing species.[49]

In addition, to obtain more reliable interaction energies, basis set superposition error (BSSE) corrections using the Boys–Bernardi counterpoise technique[50] has been calculated by the following equation

$$\Delta E_{\text{int}}^{cp}(AB) = E_{AB}^{AB}(AB) - E_{AB}^{AB}(A) - E_{AB}^{AB}(B),$$

where $E_{AB}^{AB}(AB)$ is the energy of the complex, $E_{AB}^{AB}(A)$ and $E_{AB}^{AB}(B)$ are the energy of the monomers A and B, respectively, in the complex.[51] The obtained wave functions at the B3LYP/6–311++G(d,p) computational level have been used to calculate the orbital interaction and the charge transfers within the complex framework using the NBO program[52] under Gaussian 03 package and to analyse the topological properties of the electron density within the AIM methodology[53] by AIM2000 package.[54]

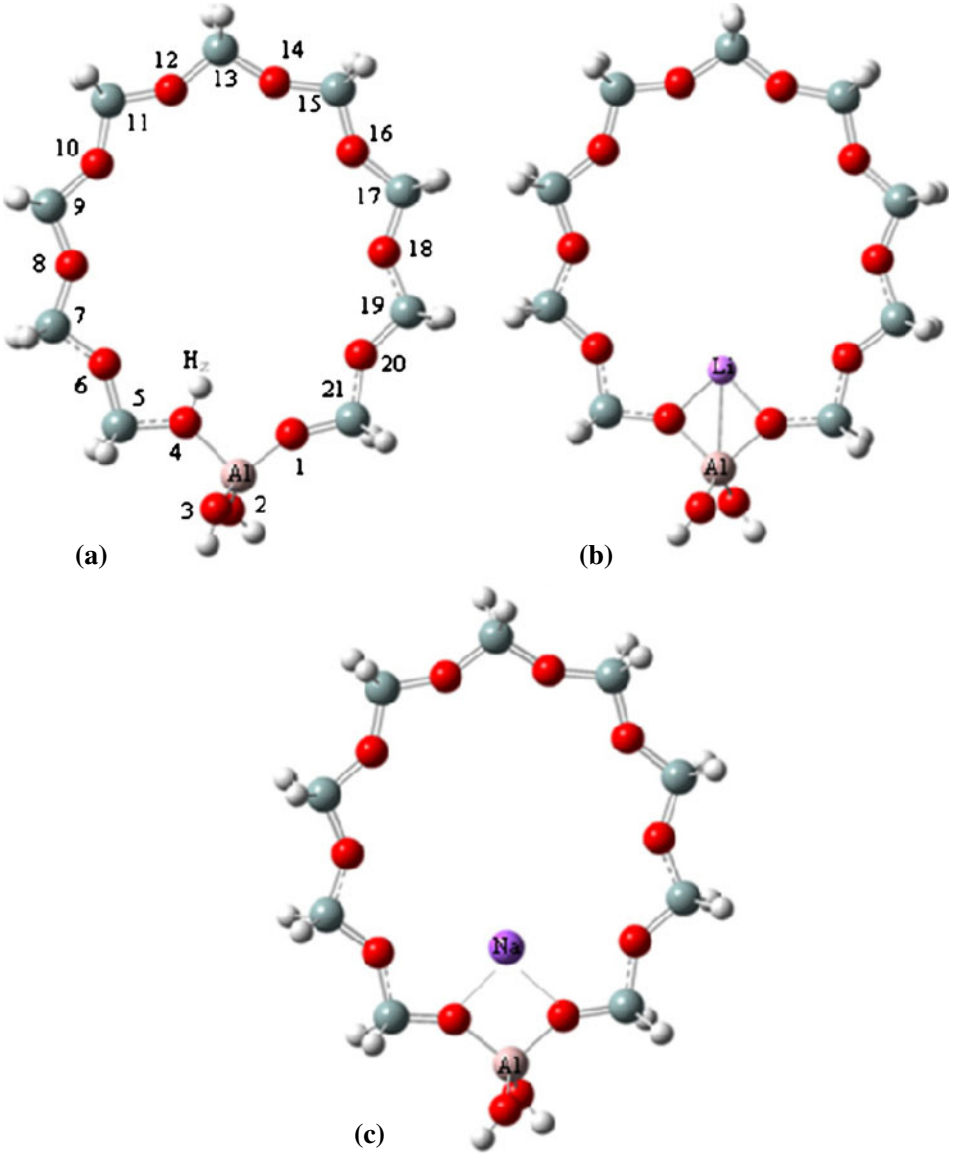

Figure 1. M-ZSM-5 cluster models: (**a**) H-zeolite, (**b**) Li-zeolite and (**c**) Na-zeolite.

3. Results and discussion

In previous study,[41] adsorption of **NA** on 10T cluster models of H-zeolite has been investigated at the different ONIOM methods. Here, we present our predictions on the effect of ion exchange on the acid strength of M-zeolite by comparing sorption energies of probe molecule **NA** in 10T cluster and comparison with H-zeolite. For this purpose, the H-zeolite complexes were optimized again without ONIOM model.

3.1 *Adsorption structures*

The optimized structures for the adsorption of the zeolite-**NA** complexes are illustrated in figures 2 and 3 while their geometric parameters are tabulated in table 1. In this work, O_Z and H_Z denote oxygen and hydrogen of ZSM-5, respectively. Two types of complexes for **NA** adsorption were considered on active sites of zeolite (with the exception of Na). In complexes **A** and **B**, oxygen and nitrogen atoms of NO group orient to the acidic H atom of H-zeolite cluster, respectively. Also, the interaction between **NA** and M-clusters (M = Li and Na) in complexes **A** and **B** occur between O(N) atom of **NA** and M atom of clusters where oxygen and nitrogen atoms of **NA** interact with active cation sites of M-zeolites, respectively. The both two types of complexes 10T cluster models were used to investigate both modes of adsorption for **NA** on Na-zeolite. But, calculations show that the only interaction between **NA** and Na-zeolite cluster occurs between

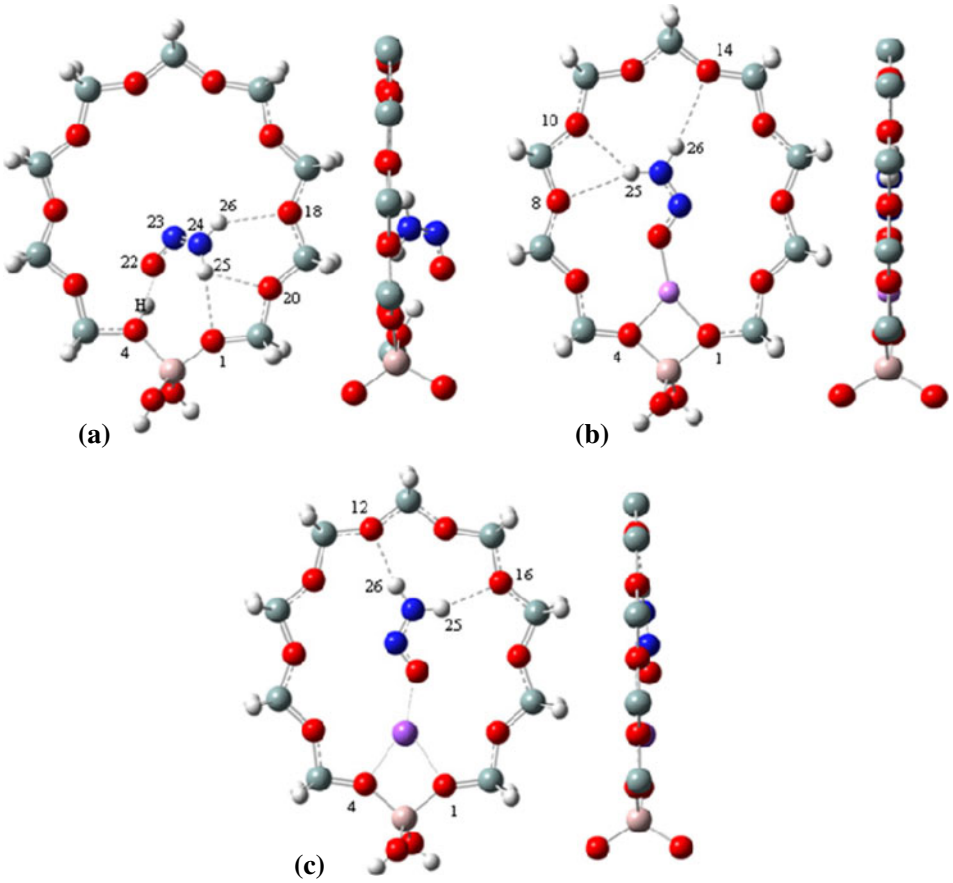

Figure 2. Front and side views of the adsorption of **NA** on M-ZSM-5 in **A** type complexes: (**a**) H-zeolite, (**b**) Li-zeolite and (**c**) Na-zeolite.

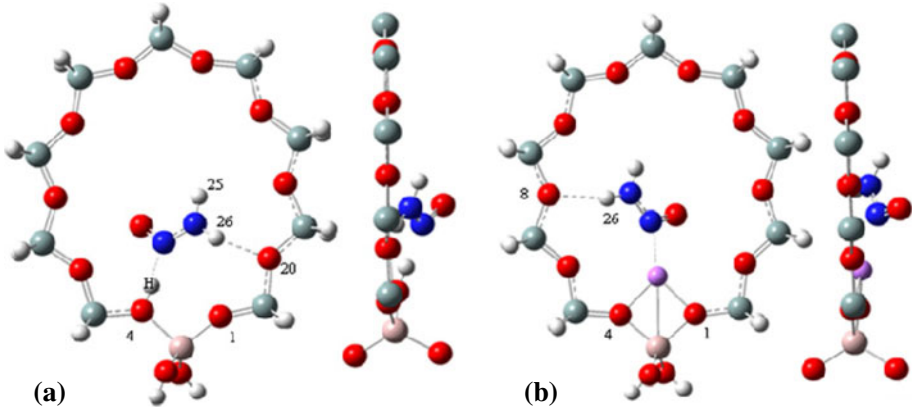

Figure 3. Front and side views of the adsorption of **NA** on M-ZSM-5 in **B** type complexes: (**a**) H-zeolite and (**b**) Li-zeolite.

O atom of **NA** and Na atom of cluster. In fact, Na has a greater tendency for adsorption of **NA** via just the O atom. In fact, the **B** complex transform to **A** one during optimization. In both **A** and **B** complexes (in all optimized M-ZSM-5 structures), observed bond critical points (BCPs) reveal that the **NA** is mainly bonded to two surface site: the acidic site M via the O and N of **NA** and the basic skeletal oxygen via the hydrogen of NH_2 group. In complexes **A** and **B**, main interaction between **NA** and cluster occurs through the O and N atoms of **NA**, respectively (see figures 2 and 3).

The **NA** adsorb on the acidic proton of H-zeolite via hydrogen bonding. The $O(N)\cdots H_Z$ interaction is the most important weak interaction between the acidic

Table 1. Selected structural parameters of the 10T cluster complexes. Bond lengths are given in angstroms and angles in degrees. The data in the parentheses correspond to monomers.

	H-zeolite		Li-zeolite		Na-zeolite
	A	**B**	**A**	**B**	**A**
Distances					
Al–O1	1.757(1.734)	1.748	1.826(1.836)	1.823	1.814(1.821)
Al–O4	1.884(1.935)	1.891	1.822(1.836)	1.831	1.815(1.821)
Si–O1	1.614(1.619)	1.607	1.649(1.655)	1.653	1.632(1.635)
Si–O4	1.696(1.715)	1.699	1.646(1.655)	1.646	1.631(1.635)
O1–M			1.987(1.896)	1.968	2.311(2.267)
O4–M			1.991(1.896)	1.967	2.304(2.267)
O4–H	1.013(0.968)	1.01			
Al$\cdots$M			2.641(2.573)	2.612	2.980(2.990)
O(N)$\cdots$M	1.616	1.726	1.915	2.09	2.222
N23–N24	1.297(1.331)	1.309	1.297	1.309	1.295
N23–O22	1.237(1.213)	1.218	1.239	1.222	1.238
N24–H25	1.023(1.018)	1.018	1.023	1.018	1.023
N24–H26	1.013(1.008)	1.019	1.013	1.015	1.014
H-bonding					
N24–H25$\cdots$$O_Z$	2.384		2.751		2.251
N24–H25$\cdots$ O_Z	2.319		2.484		
N24–H26$\cdots$$O_Z$	2.537	2.015	2.766	2.144	2.148
Angles					
<O1-A1-O4	95.6(96.5)	96.9	97.6(94.8)	97.3	101.3(40.8)
<O1-M-O4			87.3(90.9)	88.4	74.9(74.9)

site of H-cluster and **NA**. As shown in table 1, the O(N)$\cdots$$H_Z$ bond distance for **A**–**B** complexes in H-zeolite is 1.616 and 1.726 Å, respectively. The hydrogen bonding interaction lengthens the Brønsted acid O4–H_Z bond which reflects the acidic strength of the Brønsted site. Indeed, in going from **A** to **B**, O4–H_Z distance decreases as the O(N)$\cdots$$H_Z$ one increases. Increase in the O4–H_Z bond length upon complex formation of **B** (0.042 Å) is smaller than that of **A** (0.045 Å). The M$\cdots$O distance of Li-zeolite and Na-zeolite with adsorbed **NA** is 1.915 and 2.222 Å in **A** complexes, respectively. In **B** complex, the M$\cdots$N distance between nitrogen atom of **NA** and Li^+ is 2.09 Å. Thus, it is indicated that the M$\cdots$O binding distance increases slightly as the size of the alkali metal increases from Li to Na. The radius of oxygen atom is smaller than nitrogen atom, and Li$\cdots$N bond distance is longer compared to Li$\cdots$O one, indicating that the interaction between Li^+ and **NA** molecule in **A** complexes is stronger than in **B** one.

The Al$\cdots$Li and Al$\cdots$Na bond distances of M ion-exchanged zeolite complexes (M = Li and Na) with adsorbed **NA** are 2.641 and 2.980 Å in **A** type complexes, and 2.612 Å for Li-zeolite in **B** type complex, respectively. The original Al$\cdots$Li and Al$\cdots$Na bond distances of free alkali M-zeolite complexes (M = Li and Na) are 2.573 and 2.990 Å, respectively. Thus, Al$\cdots$Na bond length decreases upon complexation, while the reverse is true for the Li-zeolite. In all cases the both Si–O4 and Al–O4 bond lengths decrease upon complex formation. Decreasing of Si–O4 and Al–O4 bond length becomes lower when the cations (M^+) are changed from H^+ to Na^+. Also, change of Al$\cdots$M distance upon complexation is greater than Si–O4 and Al–O4 bond lengths in cation exchanged zeolites. Table 1 indicates that the complexation can also affects O1–Al–O4 and O1–M–O4 bond angles.

The NH$\cdots$$O_Z$ interaction is observed in all structures. In these hydrogen bonds, the N–H group of **NA** acts as donor and the zeolite oxygen framework is the acceptor. Comparison of NH$\cdots$$O_Z$ and O(N)$\cdots$$H_Z$ distances in all complexes reveals that the hydrogen bonding between hydrogen of **NA** and O_Z of framework is weaker than O(N)$\cdots$$H_Z$ (see table 1). Therefore, direct interaction between the electron acceptor group of the zeolite (such as H^+, Li^+ and Na^+) and the electron donor group of **NA** is the most important contribution to adsorption. On the other hand, in all optimized **NA**–10T structures, because of hydrogen bonding, the N–H25 and N–H26 bond lengths in **NA** increase upon complex formation and N–N bond length decreases. Increase in the N–H26 bond length is greater than N–H25 one. Because of the decrease of the electron density on N–O bond via the electron transfer from the O(N) to the M

atom, the N–O bond is elongated as a consequence of the weakening of the π bond. The original N–H25, N–H26, N–N and N–O bond distances of **NA** are 1.018, 1.008, 1.331 and 1.213 Å, respectively (see table 1).

3.2 *Adsorption energies and vibrational frequency analysis*

The calculated binding energy values for adsorption process of **NA** on the 10T cluster of M-ZSM-5 are reported in table 2 as a difference between the energy of the complex and the sum of energies of its isolated constituents. The adsorption energies of **NA** on the 10T cluster of the H-zeolite to form the **A** and **B** complexes are, respectively, −64.22 and −67.34 kJ/mol (see table 2). In previous work,[41] the calculated adsorption energies for **A** and **B** complexes were −61.30 and −65.86 kJ/mol at ONIOM(B3LYP/6–311++G(d,p):HF/3–21G(d)) level and −60.36 and −64.08 kJ/mol at ONIOM(B3LYP/6–311++G(d,p):HF/6–31+G(d)) level of theory, respectively. Our results indicate that the adsorption energy of **NA** molecule in **B** complex on the H-zeolite is larger than in **A** at the above mentioned levels, indicating that configureuration in **B** complex is more stable than that of **A**.

It is known that the H-bond strength depends on both H-bond distance and H-bond angle. Despite the H-bond distance in **A** complex of H-zeolite is smaller than **B** one, the homogenous O4–H···O H-bond angle in **A** complex (169.0°) is smaller than heterogenous O4–H···N H–bond angle in **B** one (176.5°). Thus, departure of the H-bond angle from linearity in **A** complex is greater than **B** one. Thus, small deference (∼3 kJ/mol) between absorption energy of two complexes may be attributed to difference in H-bond angles found in two complexes. Besides, change in N–N bond length upon formation of **A** complex is greater than **B** one.

As can be seen in table 2, the trend of the calculated adsorption energies for **A** type complexes is: Li-zeolite (−51.9 kJ/mol) > Na-zeolite (−35.7 kJ/mol). Also, the adsorption energy calculated for **B** complex in the Li-zeolite is −27.6 kJ/mol. These results indicate that the **A** complex is less stable than **B** in H-zeolite complexes, while the reverse is true for Li-zeolite. The comparison of energies in table 2 shows that the order of adsorption energies is Na < Li < H for **A** complexes and Li < H for **B** complexes. As a fact, the size of the cations controls the adsorption of **NA** on the M-zeolite so that smaller cations have a greater tendency for adsorption of **NA** than the larger one. The main interaction between **NA** and 10T cluster of H-zeolite occurs through hydrogen bonding. Thus, greater stability of H complex can be attributed to hydrogen bond interaction (O(N)···H_Z) in H-zeolite with respect to cation exchanged zeolites. Table 1 indicates that the O(N)···M binding distance increases slightly as the size of M increases from H to Na suggesting that the fundamental Lewis acid–base interaction weaken slightly and indicates that the **NA** which is closer to the zeolite results in the higher stabilization energy. In summary, the energetic results are in good agreement with geometric one. These results are confirmed by AIM and NBO data, which will be discussed later.

As shown in table 2, thermal and zero-point energy corrections decrease the binding energies, the stability order does not change by this corrections. Effect of thermal correction is greater than zero point.

To determine how our calculated binding energies are affected by the basis set superposition error (BSSE), we carried out counterpoise calculations at B3LYP/6–311++G(d,p) level of theory. Although the BSSE energy correction decreases the absolute values of ΔE_{elec}, the stability order does not change by this correction. For example, BSSE corrected electronic binding energy for complex **A** is −43.81 (Li-zeolite)

Table 2. Adsorption energies of NA on 10T cluster of M-ZSM-5 (kJ/mol).

complex	ΔE_{elec}	ΔE^a_{elec}	ΔE^b_0	ΔE^c	ΔH^d
NA-H-zeolite(**A**)	−64.2	−57.3	−55.7	−48.6	−51.0
NA-Li-zeolite(**A**)	−51.9	−43.8	−45.7	−38.2	−40.7
NA-Na-zeolite(**A**)	−35.7	−27.6	−28.0	−17.0	−19.5
NA-H-zeolite(**B**)	−67.3	−59.8	−59.5	−50.5	−52.9
NA-Li-zeolite(**B**)	−27.6	−20.0	−21.6	−11.9	−14.4

[a]BSSE corrected electronic energy
[b]$E_0 = E_{elec} + ZPE$
[c]$E = E_0 + E_{thermal}$
[d]$H = E_0 + H_{thermal}$

and −27.64 (Na-zeolite) kJ/mol, respectively, as given in table 2.

The heat of adsorption of a molecule interacting with a zeolite framework results not only from the chemical interaction of the reactive part of the molecule with the active site of the zeolite (by a hydrogen bond, a coordinative or chemical bond) but also from the dispersive van der Waals-type interactions of the rest of the molecule with the pore walls of zeolite, which is called non-specific interactions.[55] The calculated adsorption enthalpy (ΔH) for **A** type complexes are −51.04 kJ/mol, for H, −40.67 kJ/mol for Li and −19.52 kJ/mol, for Na. The calculated ΔH for **B** type complexes of H and Li are −52.95 and −14.41 kJ/mol, respectively. From table 2, it can be seen that the complexation enthalpy decreases in going from H^+ to Na^+, which is in agreement with increase of O(N)···M distance.

As can be seen from table 2, the size of the cations controls the adsorption of **NA** on the M-zeolite so that smaller cations (with largest electrostatic potential e/r) have a greater tendency for adsorption of **NA** than the larger one. This suggests that the cation with highest Lewis acid strength produces the strongest interaction.

The effect of the ion-exchanged alkali metal cations on the N=O, N=N and NH_2 vibrational frequencies of **NA**-zeolite complexes has been investigated. Vibrational frequencies of free **NA** and **NA** adsorbed over M-ZSM-5 calculated by DFT are shown in table 3. After adsorption, the vibrational frequencies of a molecule may shift to some extent depending on the strength of interaction with active sites. As can be seen in table 3, antisymmetric, symmetric stretching and bending vibrations of H–N–H of **NA** are appeared in the range of 3579.1–3695.2, 3393.1–3458.3 and 1578.9–1637.1 cm^{-1}, respectively. The apparent red shift of calculated antisymmetric and symmetric stretching vibrations of NH_2 group in the adsorbed state in comparison to free **NA** is attributed to hydrogen bonding of NH_2 group of **NA** via the hydrogen with oxygen atoms of cluster. Also, the amount of red-shift in NH_2 symmetric stretching vibration of **NA** is greater than asymmetric one. In addition, complexation causes elongation of O4–H_Z bond and red shift of O4–H_Z stretching vibration frequency in H-zeolites by 877.4 and 843.3 cm^{-1} upon complex formation of **A** and **B**, respectively. The experimental vibrational frequency of O4–H_Z in H-ZSM-5 is 3612.0 cm^{-1}.[56]

Compared with 1605.6 cm^{-1} of N=O bond and 1095.6 cm^{-1} of N=N bond for free **NA** molecule, the stretching frequency of N=O and N=N bond for **NA** adsorbed on M-ZSM-5 decreases and increases, respectively. Thus, complexation causes red shift of N=O and blue shift of N=N stretch frequency in cluster. These results are in agreement with the increases of N=O and decreases of N=N bond distance, as obtained from geometry optimization.

Indeed, adsorption of **NA** on cluster yields the red shifts of 94.8 (H^+), 95.1 (Li^+) and 91.4 (Na^+) cm^{-1} in **A** complexes and 22.1 (H^+) and 33.3 (Li^+) in **B** complexes for the stretching vibration of N=O from the free **NA**. Compared with the **B** complex, red shift in N=O stretching vibration of **A** is greater, which conform the changes of N=O bond distances.

3.3 *NBO analysis*

To get more specific information of adsorption **NA** on M-ZSM-5 zeolites, NBO analysis has been performed at B3LYP/6–311++G(d,p) level, which correlates well with changes in bond lengths and it provides characteristics that are closely connected to basic chemical

Table 3. Selected vibrational frequencies (cm^{-1}) calculated for 10T cluster as well as **A** and **B** complexes. The data in the parentheses correspond to the **NA**.

	H-zeolite		Li-zeolite		Na-zeolite
	A	**B**	**A**	**B**	**A**
NH_2^a	3620.3(3695.2)	3579.1	3625.4	3607.7	3596.8
NH_2^b	3399.7(3458.3)	3419.1	3410.9	3447.3	3393.1
NH_2^c	1637.1(1578.9)	1631.3	1618.4	1622.6	1634.8
O–H_Z	2911.7(3789.1)	2945.8(3612.0)[d]			
N=O	1510.8(1605.6)	1583.5	1510.5	1572.3	1514.2
N=N	1301.2(1095.6)	1291.3	1300.6	1292.3	1313.1

[a]Antisymmetric stretching
[b]Symmetric stretching
[c]Antisymmetric bending
[d]Experimental vibrational frequency of O–H in free H-ZSM-5[56]

concepts. It is used to generate information on the changes of charge densities in the bonding and antibonding orbitals. Hence, donor–acceptor (bond–antibond) interactions are taken into consideration by examining all possible interactions between filled (donor) and empty (acceptor) orbitals and then estimated their energies by second order perturbation theory. For each donor NBO(i) and acceptor NBO(j), the stabilization energy $E^{(2)}$ associated with delocalization $i \rightarrow j$ is estimated as $E^{(2)} = -q_j F^2 (i,j)/(\varepsilon_i - \varepsilon_j)$, where q_j is the donor orbital occupancy, ε_i and ε_j are diagonal elements (orbital energies) and F(i,j) is the off-diagonal NBO Fock matrix element.[51,52]

The most important NBO data are reported in table 4. As can be seen, in all cases, positive charge of the Al atom slightly increases upon complex formation so that this increase in Li-zeolite framework is greatest. The natural charge of the cations in complexes also increases when the cations are changed from H^+ to Na^+. It is also seen that the positive charge of the cations decreases upon complex formation. Thus, the bridged M atom of clusters gains electron density upon complex formation. Besides, decrease in natural charge of Li upon complex formation is greater than Na. There is a simple interpretation: because of the weaker acidity of Na^+ compared to the Li^+ ion, a further reduction of the positive charge value is observed in Li. NBO data show that the charge transfer energy corresponding to lp(O22) → lp*(M) interaction in **NA**-Li-zeolite (43.43 kcal/mol) is greater than **NA**-Na-zeolite (15.7 kcal/mol). This leads to a greater decrease of positive charge of Li with respect to Na.

The natural charges of O4 atom for **NA**-H-zeolites are found to be more than the H-zeolite comparatively. A reverse trend is observed for the alkali metal ion-exchanged zeolite complexes. Based on NBO data, there is a charge transfer interaction between valence lone pair orbital of the O4 atom and unoccupied valence non-bonding orbital of Li and Na in alkali metal exchanged zeolites. As can be seen in table 4, charge transfer energy for lp(O4) → lp*(M) interaction increases upon formation of alkali metal ion-exchanged zeolites. Thus, it is expected that negative charge of O4 atom decreases upon complex formation. This interaction is absent in H-zeolite. A common feature of all proper H-bonded complexes is the increase of electronic charge on heteroatoms.[57,58]

Inspection of NBO data shows that the charge transfer (CT) occurs from base (**NA**) to acid (M-zeolite). The CT values for **A** type complexes are 0.0827 au in H-zeolite, 0.0824 au in Li-zeolite and 0.0435 au in Na-zeolite. There is a correlation between CT values and calculated adsorption energies. Increase in CT value is accompanied with the increase in adsorption energy of **A** type complexes.

In all cases, the charge transfer between **NA** and M-zeolite is controlled by both N(O)···M interaction and NH···O_Z hydrogen bond interaction. For example, the charge transfer energies for lp(O1) → σ*(N–H25), lp(O20) → σ*(N–H25) and lp(O18) → σ*(N–H26)

Table 4. NBO results calculated at B3LYP/6−311++G(d,p) level of theory. The data in the parentheses correspond to monomers.

	H-zeolite		Li-zeolite		Na-zeolite
	A	**B**	**A**	**B**	**A**
Charge					
O22	−0.4661(−0.3887)	−0.3768	−0.4978	−0.3584	−0.5084
N23	−0.5073(−0.5730)	−0.5153	−0.4979	−0.5083	−0.5113
N24	0.2406(0.2052)	0.1616	0.2601	0.1484	0.2442
H25	0.4032(0.3682)	0.3783	0.4031	0.3874	0.4197
H26	0.4122(0.3883)	0.4314	0.4149	0.4264	0.3993
O1	−1.3475 (−1.3525)	−1.3453	−1.3573(−1.3798)	−1.3596	−1.3633(−1.3755)
O4	−1.1523(−1.1031)	−1.1536	−1.3559(−1.3798)	−1.3552	−1.3639(−1.3755)
Al	2.0933(2.0925)	2.0936	2.0774(2.0724)	2.0795	2.0837(2.0836)
M	0.5335(0.5476)	0.5314	0.8066(0.9177)	0.7725	0.8709(0.9460)
CT(NA→cluster)	0.0827	0.0793	0.0824	0.0955	0.0435
$E^{(2)}$/kcal mol^{-1}					
π(N=O) → lp*(M)			5.07	5.04	2.21
π*(N=O) → lp*(M)			0.51	1.88	0.34
lpN(O) → lp*(M)			43.43	31.61	15.7
lpO_Z → σ*(N–H25)	2.2		0.44		3.24
lpO_Z → σ*(N–H25)	0.07		1.12		
lpO_Z → σ*(N–H26)	0.76	6.96	0.38	4.31	4.46

interactions in **A** complex of H-zeolite are 2.2, 0.07 and 0.76 kcal/mol, respectively, and that of lp(O20) → σ*(N–H26) interactions in complex **B** is 6.96 kcal/mol. These interactions also have an important role on the stability of Li and Na complexes. A common property of all complexes is the decrease of electronic charge on the both bridging H25 and H26 hydrogen atoms.

For **NA** adsorbed on the Brønsted acid of alkali metal exchanged zeolites, NBO calculations show that the charge transfers are also due to the orbital interaction between the σ bonding (donor) orbital of the N=O bond of **NA** with lp*(M) orbital of alkali metal zeolites. From table 4, the charge transfer energy associated with the π(N=O) → lp*(M) interaction for **A** type complex is as follows: Li (5.07 kcal/mol) > Na (2.21 kcal/mol). The presence of π(N=O) → lp*(M) interactions in alkali metal ion-exchanged zeolites, resulting in the lengthening of the N=O bond as a consequence of the weakening of the π bond of the **NA**. The fact that, the less the bonds order, the longer the bonds distance and vice versa, is attributed to the loss of electron occupancy in the bonding orbital and the gain in electron occupancy in the antibonding orbital.[10]

Also, based on NBO analysis, it was found that the most significant donor–acceptor stabilization between cation and the adsorbate molecules in alkali metal exchanged zeolites comes from the interaction between a valence lone pair orbital of the O(N) atoms of the adsorbed molecule that are oriented towards the cations and an unoccupied valence non-bonding orbital of Li and Na. As mentioned above, charge transfer energy for lp(O) → lp*(Li) and lp(O) → lp*(Na) interactions in complex **A** are 43.43 and 15.7 kcal/mol and that of lp(N) → lp*(Li) interaction in complex **B** is 31.61 kcal/mol, respectively. Consequently, as the value of $E^{(2)}$ increases [π(N=O) → lp*(M) and lp(O or N) → lp*(M)] in alkali metal exchanged zeolites, a greater amount of charge is transferred, and the M–O(N) bond length decreases, as would be expected.

3.4 *AIM analysis*

The Bader's[53] atoms in molecules (AIM) theory is a powerful tool to analyse molecular structures and intermolecular interactions and give much more detailed information on the nature of electron distribution in the molecules.[59,60] The use of this theory makes it possible to solve and understand many chemical and physical problems. In the quantum theory of atoms in molecules (QTAIM) analyses, the nature of a bonding interaction can be determined through an analysis of the properties of charge density, ρ, and its Laplacian, $\nabla^2\rho$, at the bond critical point, and through the properties of the atoms, which are obtained by integrating the charge density over the atomic basin. The properties calculated at the bond critical point include the total electron density, ρ, which has been related to bond order, Laplacian of charge density, $\nabla^2\rho$, which measures the extent to which density is concentrated or depleted (more negative $\nabla^2\rho$ indicates the greater concentration of charge), kinetic energy density (G), energy density (H) and the bond ellipticity (ε) which is often taken as a measure of π-bond character.[53,61,62] Unlike the Laplacian, whose sign is determined by the local virial expression,[63] the sign of H_{BCP} is determined by the energy density itself.

The values of electron density (ρ), Laplacian of electron density ($\nabla^2\rho$) and total energy density (H_{BCP}), were evaluated at the bond critical points (BCPs) by the means of AIM approach at the B3LYP/6–311++G(d,p) level of theory. Inspection of molecular graphs and contour plates indicates the presence of a critical point at O(N)···M (M = H, Li and Na) BCP, indicating the interaction between **NA** and zeolites. An examination of the electron density and geometry compared to purely clusters shows similar features for all complexes.

The comparison of AIM data for **NA** with corresponding values calculated at MP2/6–311++G(2d,2p) level of theory[64] should be interesting. The values of ρ at N–N and N=O BCPs of **NA** at MP2/6–311++G(2d,2p) level of theory are 0.3799 and 0.4867 au, respectively. Also, the $\nabla^2\rho$ and H values are −0.6305 and −0.3534 au for N–N BCP and −0.9174 and −0.5780 au for N=O BCP, respectively. Besides, ρ and $\nabla^2\rho$ and H values calculated at MP2/6–311++G(2d,2p) level of theory at N–H BCP of **NA** are 0.3446, −1.8143 and −0.5076 au, respectively. Comparison of AIM data calculated at two levels of theory show that the AIM data are sensitive to level of theory. In comparison with the MP2/6–311++G(2d,2p) level of theory, B3LYP/6–311++G(d,p) level of theory overestimate AIM data of N–N and N=O BCPs. However, in this work, the change in AIM data upon complexation, which is less sensitive to level of theory, was investigated.

As can be seen in table 5, electron density at O4–H_Z BCP of the model cluster of H-zeolite decreases upon complexation. For this BCP, $\nabla^2\rho$ and H_{BCP} are negative, indicating its covalent character. In addition, complexation causes the decrease in the covalent nature of O4–H_Z in both **A** and **B** complexes. Also, values of $\nabla^2\rho$ and H_{BCP} at O(N)···H_Z BCP of complexes are positive and negative, respectively, indicating the accumulation of electron density at the associated BCPs. Bonds with positive value of $\nabla^2\rho$ and small negative value of H_{BCP} at BCP are termed as partially covalent in nature. The

Table 5. Calculated BCP data (au) for NA-M-ZSM-5 complexes at B3LYP/6–311++G(d,p) level of theory. The data in the parentheses correspond to monomers.

Bond	ρ(r)	$\nabla^2\rho$	H(r)	ρ(r)	$\nabla^2\rho$	H(r)
		NA-H-zeolite(**A**)			NA-H-zeolite(**B**)	
Al–O1	0.0841(0.0893)	0.6969(0.7590)	0.0072(0.0070)	0.0857	0.7186	0.0075
Al–O4	0.0601(0.0521)	0.4450(0.3687)	0.0075(0.0067)	0.0590	0.4333	0.0073
H–O4	0.2984(0.3473)	−1.9673(−2.4586)	−0.5588(−0.6773)	0.3002	−1.9817	−0.5622
O–N	0.4802(0.5122)	−1.1215(−1.2821)	−0.6195(−0.7011)	0.5053	−1.2064	−0.6747
N–N	0.4214(0.3887)	−0.9658(−0.7910)	−0.4688(−0.4017)	0.4085	−0.8947	−0.4405
N–H25	0.3270(0.3303)	−1.6844(−1.6040)	−0.4651(−0.4505)	0.3317	−1.6509	−0.4598
N–H26	0.3379(0.3412)	−1.7737(−1.7247)	−0.4876(−0.4804)	0.3301	−1.7909	−0.4910
Hz···O(N)	0.0550	0.1376	−0.0098	0.0501	0.0965	−0.0100
H26···O18	0.0074	0.0251	0.0009			
H25···O1	0.0106	0.0334	0.0011			
H25(H26)···O20	0.0136	0.0499	0.0015	0.0217	0.0787	0.1003
		NA-Li-zeolite(**A**)			NA-Li-zeolite(**B**)	
Al–O1	0.0711(0.0696)	0.5426(0.5246)	0.0064(0.0062)	0.0717	0.5480	0.0063
Al–O4	0.0719(0.0696)	0.5515(0.5246)	0.0065(0.0062)	0.0702	0.5337	0.0064
Li–O1	0.0258(0.0328)	0.1773(0.2422)	0.0075(0.0101)	0.0274	0.1893	0.0079
Li–O4	0.0255(0.0328)	0.1757(0.2422)	0.0075(0.0101)	0.0270	0.1900	0.0082
O–N	0.4794	−1.1218	−0.6167	0.5016	−1.1849	−0.6652
N–N	0.4216	−0.9706	−0.4692	0.4082	−0.8953	−0.4395
N–H25	0.3267	−1.6730	−0.4616	0.3315	−1.6617	−0.4618
N–H26	0.3374	−1.7808	−0.4887	0.3333	−1.7906	−0.4913
Li···O(N)	0.0291	0.2135	0.0099	0.0226	0.1379	0.0061
H26···O14	0.0041	0.0144	0.0007			
H25···O10	0.0083	0.0277	0.0010			
H25(H26)···O8	0.0044	0.0160	0.0008	0.0165	0.0586	0.0018
		NA-Na-zeolite(**A**)				
Al–O1	0.0727(0.0716)	0.5667(0.5527)	0.0071(0.0069)			
Al–O4	0.0724(0.0716)	0.5642(0.5527)	0.0071(0.0069)			
Na–O1	0.0220(0.0245)	0.1371(0.1569)	0.0055(0.0062)			
Na–O4	0.0224(0.0245)	0.1401(0.1569)	0.0056(0.0062)			
O–N	0.4805	−1.1189	−0.6180			
N–N	0.4239	−0.9834	−0.4740			
N–H25	0.3271	−1.6679	−0.4613			
N–H26	0.3364	−1.7982	−0.4936			
Na···O	0.0256	0.1733	0.0075			
H26···O12	0.0160	0.0573	0.0018			
H25···O16	0.0131	0.0444	0.0014			

electron density at O4–H_Z BCP correlates well with that of O(N)···H_Z BCP. Increase in electron density of O(N)···H_Z BCP is accompanied with decrease of O4–H_Z BCP. This is associated with the transfer of electron charge from the Lewis base (**NA**) to Lewis acid (zeolite) as a consequence of complexation.

In all complexes, $\nabla^2\rho$ and H_{BCP} values at O4–Al BCP are positive; this is an indication of electrostatic nature of this bond. The ρ, Laplacian and H_{BCP} values at O4–Al BCP increase upon complexation, in consistence with decrease of its bond distance. From these values, it can be predicted that the electrostatic nature of O4–Al bond increases upon complexation. The values of ρ and $\nabla^2\rho$ at O1–Al BCP decrease upon complexation in H-zeolite. The observations are reversed for the alkali metal ion-exchanged zeolites. On the other hand, in alkali metal cation exchanged zeolites, ρ, $\nabla^2\rho$ and H_{BCP} values at O4–M BCP decrease upon complexation. In this BCP, $\nabla^2\rho$ and H_{BCP} values are also positive. A similar behaviour is observed for the mentioned values at O1–M BCP (see table 5).

As shown in table 5, all $\nabla^2\rho$ and H_{BCP} values at M···O(N) (M = Li and Na) BCP of complexes are positive, which indicate they have properties of electrostatic interactions. The charge density, $\nabla^2\rho$ and H_{BCP} at M···O(N) BCP decrease on going from complex Li to complex Na. This decrement is consistent with the elongation of the M···O(N) distance. In these complexes the ρ and $\nabla^2\rho$ values at O(N)···M BCP in Li-zeolite are greater than those of Na-zeolite, in agreement with

greater charge transfer upon π(N=O) $\rightarrow$ lp*(M) and lp(O or N) $\rightarrow$ lp*(M) interaction from **NA** to zeolite. Thus, it confirms the results of the structural parameters and NBO data that the O(N)$\cdots$M interaction in Li complex is stronger than Na. Also, The values of ρ, $\nabla^2\rho$ and H_{BCP} at M$\cdots$O(N) BCP in Li-zeolite in the **A** complex are higher than those in the **B** one, in agreement with the energetic prediction.

Inspection of QTAIM data corresponding to the **NA**–10T complexes reveals the presence of critical point at NH$\cdots O_Z$ (M = H, Li and Na) BCP, indicating the additional interaction between **NA** and zeolites. Electron density at NH$\cdots O_Z$ BCP in all complexes is smaller than M$\cdots$O(N) BCP one, showing its weaker interaction. BCP data for NH$\cdots O_Z$ bond are positive, in consistence with the most common feature of hydrogen bonding contacts. This means that the NH$\cdots O_Z$ interactions have electrostatic nature. The comparison of BCP data of N–H26 and N=O bonds in the **A** and **B** complexes with those of monomer **NA** in all clusters (table 5) shows that the charge density at BCPs decreases upon hydrogen bonding, in agreement with the increase of its bond distance, while the reverse is true for the N=N bond. Besides, O=N has covalent nature that increases upon complexation.

4. Conclusions

The adsorption of parent nitrosamine on the M-ZSM-5 was investigated by B3LYP density functional calculations using 10T-membered ring cluster to model the Brønsted acid sites of zeolite. This is a study to monitor the role of exchangeable cations on the activity of zeolites. Two types complexes (**A**–**B**) were predicted from adsorption of nitrosamine on the M-zeolite clusters (Na excepted). The acid strength of H-ZSM-5 was found to exceed those of the alkali metal ion-exchanged zeolites. The comparison of binding energies shows that the order of adsorption energies is Na < Li < H for the **A** type complexes and Li < H for the **B** type complexes. Also, the adsorption energy of **NA** on H-zeolite in **B** complex is slightly larger than **A**. A reverse trend is observed for Li-zeolite complexes.

The positive natural charges of the M decrease upon complex formation in M-zeolite. The natural charge of the cations also increases when the cations are changed from H^+ to Na^+. The calculated natural charges showed that charge transfer occurs from base (**NA**) to acid (zeolite) upon complex formation.

The main interaction between **NA** and 10T cluster of M-zeolites occurs through the O(N)$\cdots H_Z$ interactions. Also, the NH$\cdots O_Z$ interactions have important role in stability of complexes. The comparisons of BCPs data and bond distances of O(N)$\cdots H_Z$ with NH$\cdots O_Z$, reveal that the hydrogen bonding between hydrogen of **NA** and O_Z of framework is weaker than O(N)$\cdots H_Z$ interaction. The NH$\cdots O_Z$ and O(N)$\cdots H_Z$ hydrogen bonds in these complexes are electrostatic and partially covalent in nature, respectively.

References

1. Wu Z Y, Wang H J, Ma L L, Wue J and Zhu J H 2008 *Micropor. Mesopor. Mat*. **109** 436
2. Myburg R B, Dutton M F and Chuturgoon A A 2002 *Environ. Health Persp*. **110** 813
3. Bartsch H, Ohshima H, Pignatelli B and Camels S 1989 *Cancer Surv*. **8** 335
4. Yun Z Y, Xu Y, Xu J H, Wu Z Y, Wei Y l, Zhou Z P and Zhu J H 2004 *Micropor. Mesopor. Mater*. **72** 127
5. Preussmann R 1981 *Public health significance of environmental N-nitroso compounds* H Egan (ed.) Environmental Carcinogens: Selected Methods of Analysis. Vol. 6. N-Nitroso Compounds. IARC Scientific Publication, Lyon, France: International Agency for Research on Cancer, vol. 45, p. 3
6. Hecht S S 1999 *Mutat. Res*. **424** 127
7. Zhou C F, Cao Y, Zhuang T T, Huang W and Zhu J H 2007 *J. Phys. Chem. C* **111** 4347
8. Davis D L and Nielsen M T (eds) 1999 *Tobacco: production, chemistry and technology*, London: Blackwell Sciences
9. Auerbach S M, Carrado K A and Dutta P K 2003 *Hand book of zeolite science and technology*, New York: Marcel Dekker. Inc
10. Namuangruka S, Tantanak D and Limtrakul J 2006 *J. Mol. Catal. A: Chemical* **256** 113
11. Vollmer J M, Stefanovich E V and Truong T N 1999 *J. Phys. Chem. B* **103** 9415
12. Solans-Monfort X, Sodupe M, Branchadell V, Sauer J, Orlando R and Ugliengo P 2005 *J. Phys. Chem. B* **109** 3539
13. Roohi H and Azarpour M 2008 *Micropor. Mesopor. Mater.* **113** 240
14. Kassab E, Castella-Ventura M and Akacem Y 2009 *J. Phys. Chem. C* **113** 20388
15. Treesukol P, Limtrakul J and Truong T N 2001 *J. Phys. Chem. B* **105** 2421
16. Wang Y, Lei Z, Zhang R and Chen B 2010 *J. Mol. Struct. (Theochem)* **957** 41
17. Sung C Y, Broadbelt L J and Snurr R Q 2008 *Catalysis Today* **136** 64
18. Arean C O, Delgado M R, Frolich K, Bulanek R, Pulido A, Bibiloni G F and Nachtigall P 2008 *J. Phys. Chem. C* **112** 4658
19. Limtrakul J, Jungsuttiwong S and Khongpracha P 2000 *J. Mol. Struct. (Theochem)* **525** 153
20. Chatterjee A, Ebina T, Iwasaki T and Mizukami F 2003 *J. Mol. Struct. (Theochem)* **630** 233
21. Agarwal V, Jr W C C and Auerbach S M 2011 *J. Phys. Chem. C* **115** 188

22. Chatterjee A and Mizukami F 2004 *Chem. Phys. Lett*. **385** 20
23. Treesukol P, Srisuk K, Limtrakul J and Truong T N 2005 *J. Phys. Chem. B* **109** 11940
24. Bludsky O, Silhan M, Nachtigallova D and Nachtigall P 2003 *J. Phys. Chem. A* **107** 10381
25. Yang J, Zhou Y, Wang H J, Zhuang T T, Cao Y, Yun Z Y, Yu Q and Zhu J H 2008 *J. Phys. Chem. C* **112** 6740
26. Rozanska X, Barbosa L A M M and van Santen R A 2005 *J. Phys. Chem. B* **109** 2203
27. Jiang S, Huang S, Qin L, Tu W, Zhu J, Tian H, Wang P 2010 *J. Mol. Struct. (Theochem)* **962** 1
28. Vankoningsveld H 1990 *Acta Crystallogr. Sec. B – Struct. Sci.* **46** 731
29. Kucera J, Nachtigall P, Kotrla J, Kosova G and Cejka J 2004 *J. Phys. Chem. B* **108** 16012
30. Sierraalta A, Alejos P, Ehrmann E, Rodriguez L J and Ferrer Y 2009 *J. Mol. Catal. A: Chemical* **301** 61
31. Areán C O, Delgado M R, Frolich K, Bulánek R, Pulido A, Bibiloni G F and Nachtigall P 2008 *J. Phys. Chem. C* **112** 4658
32. Qiu Z Z, Yu Y X, Mi J G 2012 *Appl. Surface Sci.* **258** 9629
33. Xu Y, Yun Z Y, Zhu J H, Xu J H, Liu H D, Wei Y L and Hui K J 2003 *Chem. Commun.* 1894
34. Zhu J H, Yan D, Xia J R, Ma L L and Shen B 2001 *Chemosphere* **44** 949
35. Zhou C F and Zhu J H 2005 *Chemosphere* **58** 109
36. Zhou C F, Yun Z Y, Xu Y, Wang Y M, Chen J and Zhu J H 2004 *New J. Chem*. **28** 807
37. Cao Y, Yun Z Y, Yang J, Dong X, Zhou C F, Zhuang T T, Yu Q, Liu H D and Zhu J H 2007 *Micropor. Mesopor. Mater*. **103** 352
38. Xu Y, Zhu J H, Ma L L, Ji A, Wei Y L and Shang X Y 2003 *Micropor. Mesopor. Mater*. **60** 125
39. Gu F N, Zhuang T T, Cao Y, Zhou C F and Zhu J H 2008 *Solid State Sci*. **10** 1658
40. Xu Y, Yun Z Y, Zhou C F, Zhou S L, Xu J H and Zhu J H 2004 *Stud. Surf. Sci. Catal*. **154** 1858
41. Roohi H and Akbari F 2010 *Appl. Surface Sci.* **256** 7575
42. Redondo A and Hay P J 1993 *J. Phys. Chem*. **97** 11754
43. van Koningsveld H, van Bekkum H and Jansen J 1987 *Acta. Crystallogr. B* **43** 127
44. van Koningsveld H, van Bekkum H and Jansen J 1990 *Zeolites* **10** 235
45. Sirijaraensre J, Truong T N and Limtrakul J 2005 *J. Phys. Chem. B* **109** 12099
46. Frisch M J, Trucks G W, Schlegel H B, Scuseria G E, Robb M A, Cheeseman J R, Montgomery J A J r, Vreven T, Kudin K N, Burant J C, Millam J M, Iyengar S S, Tomasi J, Barone V, Mennucci B, Cossi M, Scalmani G, Rega N, Petersson G A, Nakatsuji H, Hada M, Ehara M, Toyota K, Fukuda R, Hasegawa J, Ishida M, Nakajima T, Honda Y, Kitao O, Nakai H, Klene M, Li X, Knox J E, Hratchian H P, Cross J B, Adamo C, Jaramillo J, Gomperts R, Stratmann R E, Yazyev O, Austin A J, Cammi R, Pomelli C, Ochterski J W, Ayala P Y, Morokuma K, Voth G A, Salvador P, Dannenberg J J, Zakrzewski V G, Dapprich S, Daniels A D, Strain M C, Farkas O, Malick D K, Rabuck A D, Raghavachari K, Foresman J B, Ortiz J V, Cui Q, Baboul A G, Clifford S, Cioslowski J, Stefanov B B, Liu G, Liashenko A, Piskorz P, Komaromi I, Martin R L, Fox D J, Keith T, Al-Laham M A, Peng C Y, Nanayakkara A, Challacombe M, Gill P M W, Johnson B, Chen W, Wong M W, Gonzalez C and Pople J A 2003 Gaussian03 (Revision B03) Gaussian, Inc, Pittsburgh, PA
47. Solans-Monfort X, Bertrain J, Branchadell V and Sodupe M 2002 *J. Phys. Chem. B* **106** 10220
48. Joshi Y V and Thomson K T 2008 *J. Phys. Chem. C* **112** 12825
49. Bates S P and van Santen R A 1998 *Adv. Catal*. **42** 1
50. Boys S F and Bernardi F 1990 *Mol. Phys*. **19** 553
51. Kolandaivel P and Nirmala V 2004 *J. Mol. Struct*. **694** 33
52. Reed A E, Curtiss L A and Weinhold F 1988 *Chem. Rev*. **88** 899
53. Bader R F W 1990 *Atoms in molecules: a quantum theory*, Oxford UK: Clarendon Press
54. Biegler-König F, Schönbohm J and Bayles D 2001 *J. Comp. Chem*. **22** 545
55. Vayssilov G N, Lercher J A and Rösch N 2000 *J. Chem. Phys. B* **104** 8614
56. Kotrla J, Nachtigallova D and Kubelkova L 1998 *J. Phys. Chem. B* **102** 2454
57. Zeegers-Huyskens T 2003 *J. Phys. Chem. A* **107** 8730
58. Grabowski S J (ed.) 2006 *Hydrogen bonding–new insights*, Dordrecht: Springer
59. Koch U and Popelier P L A 1995 *J. Phys. Chem*. **99** 9747
60. Popelier P L A 1998 *J. Phys. Chem. A* **102** 1873
61. Bader R F W and Essen H 1994 *J. Chem. Phys*. **80** 1943
62. Bader R F W 1991 *Chem. Rev*. **91** 893
63. Bader R F W 1998 *Can. J. Chem*. **76** 973
64. Roohi H, Nowroozi A R and Anjomshoa E 2011 *Comp. Theo. Chem*. **965** 211